Superconducting proximity effects in metals with a repulsive pairing interaction

Oriol T. Valls* and Matthew Bryan†
School of Physics and Astronomy, University of Minnesota, Minneapolis, Minnesota 55455, USA

Igor Žutić‡
Department of Physics, University at Buffalo, Buffalo, New York 14260, USA
(Received 11 June 2010; published 27 October 2010)

Studies of the superconducting proximity effect in normal conductor/superconductor (N/S) junctions almost universally assume no effective electron-electron coupling in the N region. While such an approximation leads to a simple description of the proximity effect, it is unclear how it could be rigorously justified. We reveal a much more complex picture of the proximity effect in N/S bilayers, where S is a clean s-wave BCS superconductor and N is a simple metal with a repulsive effective electron coupling. We elucidate the proximity effect behavior using a highly accurate method to self-consistently solve the Bogoliubov-deGennes equations. We present our results for a wide range of values of the interface scattering, the Fermi wave-vector mismatch, the temperature, and the ratio g of the effective interaction strengths in the N and S regions. We find that the repulsive interaction, represented by a negative g, strongly alters the signatures of the proximity effect as can be seen in the spatial dependence of the Cooper pair amplitude and the pair potential, as well as in the local density of states near the interface.

DOI: 10.1103/PhysRevB.82.134534 PACS number(s): 74.45.+c, 74.78.Fk, 74.78.Na

I. INTRODUCTION

For nearly eight decades it has been recognized that superconducting properties can leak out from a superconductor into a neighboring metallic region[1–3] which by itself would not be superconducting. This phenomenon is known as the superconducting proximity effect. That superconductivity can penetrate into a nonsuperconductor for a long distance,[2] has fascinated the condensed-matter community ever since this was discovered.

The main signatures of the proximity effect include the penetration of the Cooper pairs, with associated phase coherence, into the nonsuperconducting region, and the suppression of the pair potential (the superconducting order parameter) in the superconductor, near the interface. Important insights in the proximity effect[4,5] are provided by its connection to the process of Andreev-Saint James reflection.[6–11] An incident electron approaching a normal metal/superconductor (N/S) interface from the N region can be reflected as a hole, resulting in the transfer of a Cooper pair into the S region. This is a phase-coherent scattering process in which the reflected particle carries information about both the phase of the incident particle and the macroscopic phase on the superconductor.[12] Thus, Andreev reflection is responsible for introducing phase coherence in the normal region. Since this reflection is a two-particle process, it is plausible to conclude that the proximity effect will be also weaker whenever this anomalous reflection is suppressed, as, e.g., in low-transparency N/S junctions.

Very impressive advances in the fabrication of superconducting junctions (including atomically flat interfaces[13]) have in recent years stimulated extensive experimental and theoretical studies of the proximity effect. For example, many recent efforts have focused on elucidating proximity effects in junctions including ferromagnets[14–18] or superconductors with unconventional (non-s-wave) pairing symmetry.[6,19,20] However, significant challenges remain even for the studies of the proximity effect in a simple N/S junction, where N is the normal conductor and S is a conventional BCS superconductor with phonon-mediated s-wave pairing symmetry. One such issue is that of the role of the effective pairing interaction in the N material. In the simplest BCS version of the theory, the S region is characterized by a coupling constant λ conventionally taken as positive for the attractive case. In nearly all of the standard treatments of the S/N proximity effect this constant is assumed to vanish in the N region.[21] This implies that the pair potential, which enters in the underlying microscopic equations, would completely vanish in the N region (although the pair amplitude would not) for any choice of the N region and the N/S interface. Yet, this zero coupling assumption is hardly realistic: while the low-frequency phonon mediated interaction is, on general grounds, always attractive, the coupling λ represents the difference between this attraction and the Coulomb pseudopotential, which is invariably repulsive. The balance of the two quantities may lead to a positive λ, leading to superconductivity, or a negative λ but it is most unlikely that the two would exactly cancel. Indeed one would expect, in nonsuperconductors, negative values of λ in roughly the same absolute value range of those found in superconductors.

This was already noted a long time ago[22] in a review article by de Gennes[7] and it was implicit in even earlier work.[23] The idea was extensively followed up at the time: the comprehensive review article[2] mentioned above discussed and reviewed many important aspects of proximity effect phenomena with emphasis on issues that could be tackled at the time. The contemporary constraints were both experimental and theoretical, implied by the quality of the samples and interfaces then available, the absence of suitable high-resolution probes such as the scanning tunneling microscope, and the limited capacity of the existing computers, which largely restricted theory to analytic methods. Among other topics, in Ref. 2 the effect on T_c of an attractive or repulsive interaction in the N material was considered, with more em-

phasis on the attractive case; a version of the so-called "Cooper limit"[23] argument, for dirty superconductors and thin N and S layers, already given in Ref. 22, was presented; and a qualitative account of the energy-gap behavior at an N/S interface was included.[24] As further follow up to these reviews, additional work, including, e.g., several experiments[25–28] that used electromagnetic and transport properties to estimate the pairing interaction and its sign, were subsequently performed in the early seventies. Yet, despite the wide dissemination of these reviews and the high reputation of their authors, activity on this problem eventually dwindled and relatively little attention has been paid for many years to the question of the influence of a *negative* value of λ in the N material, on the proximity effect. The work of Refs. 29 and 30, restricted to the quasiclassical limit, and that of Ref. 31 on critical currents in the Cooper limit are among the few exceptions. The unspoken assumption elsewhere seems to have been that provided λ is nonpositive its value does not matter. Yet, as pointed out already in Ref. 22, such an assumption is quite unreasonable. A repulsive interaction in the N region will tend to break the Cooper pairs coming from the S region, which are responsible for the proximity effect. The situation might be in some ways reminiscent of that found in the ferromagnet/superconductor (F/S) proximity[14] effect for a weak ferromagnet, where the range of the effect is reduced and signatures are found in the local density of states (LDOS) due to modified Andreev reflection and Andreev-Saint James states.[7]

In this work we reexamine this long-standing question in a rigorous way. We do this by solving the relevant microscopic equations, the Bogoliubov-de Gennes[32] equations, in a fully self-consistent way, using computational methods recently developed and applied[33,34] to study several aspects of the F/S proximity effects in clean systems with smooth interfaces. We consider an N/S bilayer in which each layer is thicker than the superconducting coherence length, ξ_0, in the S material, and we study the properties of the system, focusing particularly on both the Cooper pair amplitude and the pair potential as a function of position, as well as on the LDOS near the interface. We study the problem for several values of the interface scattering, the Fermi wave vector mismatch between the two materials and, most important, of the value of the *nonpositive* ratio g between the effective pairing constant λ_N on the N side and the positive value λ_S on the S side. We find that the proximity effect markedly depends on g with the penetration of the pair amplitude into N being reduced as the absolute value of g increases. There is even a "negative" proximity effect: the presence of a repulsive interaction in the normal metal depletes the pair amplitude in S near the interface. There are also signatures of the g dependence on the LDOS as measured very near the interface. Not surprisingly, these signatures are different from those apparent in the quasiclassical[29] approximation, which cannot be accurate at very small length scales.[35] As a useful byproduct of our computations, we find that it is erroneous, in the study of the N/S proximity effect, to subsume the separate effects of interfacial scattering and wave vector mismatch into a single effective parameter. This has been long known[36–38] to be the case for F/S interfaces but the situation in the N/S case was still unclear.

II. METHODS

To study this problem, we solve self-consistently the Bogoliubov-deGennes (BdG) equations,[32] the relevant microscopic description for a clean system. The geometry we consider consists of one normal-metal slab of thickness d_s juxtaposed to a similar slab of an ordinary BCS superconductor of thickness d_S. We assume a flat interface of arbitrary transparency, infinite in the x and y directions while the z axis is normal to the interface. The methods we use here have been presented and discussed elsewhere[33,34,38–41] and details need not be given again here. In this geometry the BdG equations can be written as

$$\begin{pmatrix} H & \Delta(z) \\ \Delta(z) & -H \end{pmatrix} \begin{pmatrix} u_n^{\uparrow}(z) \\ v_n^{\downarrow}(z) \end{pmatrix} = \epsilon_n \begin{pmatrix} u_n^{\uparrow}(z) \\ v_n^{\downarrow}(z) \end{pmatrix} \tag{2.1}$$

in terms of the spin-up quasielectron, $u_n^{\uparrow}(z)$, and spin-down quasihole, $v_n^{\downarrow}(z)$, amplitudes. Here $\Delta(z)$ is the pair potential (order parameter[42]) which is to be determined self-consistently as explained below. The single-particle Hamiltonian is

$$H = k_z^2/2m + \epsilon_{\perp} + U(z) - E_F(z), \tag{2.2}$$

where $k_z^2/2m$ and $\epsilon_{\perp} = k_{\perp}^2/2m$, denote the kinetic energy from motion in the z and $x-y$ direction for parabolic bands, respectively, $U(z)$ is a scalar potential and $E_F(z)$ represents the Fermi energies (band widths) E_{FN}, E_{FS} in the N and S regions. We set $\hbar = k_B = 1$, for Planck's and Boltzmann's constants. The variables $\epsilon_{\perp}$ are decoupled from the z direction but they affect the eigenvalues ϵ_n. These variables are measured from the chemical potential. As pointed out already in many places,[33,34,37–39] one should not assume in this type of problem that the Fermi wave vectors k_{FN} and k_{FS} (or, equivalently, E_{FN}, E_{FS}, as measured from the bottom of the bands) are the same in both materials. Thus, we introduce a dimensionless mismatch parameter defined as

$$\Lambda \equiv E_{FN}/E_{FS} = (k_{FN}/k_{FS})^2. \tag{2.3}$$

We characterize the mismatch by this single parameter without the additional introduction of different effective masses in the N and S regions,[43] which would not alter our findings. In Eq. (2.2) we choose the scalar potential to describe the interfacial scattering $U(z) = H_0 \delta(z - z_0)$, where z_0 is the location of the interface. The strength of this scattering is conveniently given in terms of the dimensionless barrier strength $H_B \equiv m H_0 / k_{FS}$, which in the limit of no mismatch ($\Lambda = 1$), coincides with the parameterization introduced in Ref. 10.

The BdG Eqs. (2.1) above must be solved together with the self-consistency condition

$$\Delta(z) = \frac{\lambda(z)}{2} \sum_n{}' [u_n^{\uparrow}(z) v_n^{\downarrow}(z) + u_n^{\downarrow}(z) v_n^{\uparrow}(z)] \tanh\left(\frac{\epsilon_n}{2T}\right), \tag{2.4}$$

where $\lambda(z) = \lambda_N < 0$ and $\lambda(z) = \lambda_S > 0$ in the N and S regions, respectively, the prime in the summation sign indicates that it is limited by the usual Debye cutoff, and T is the absolute temperature.

The procedures to diagonalize the BdG numerically while ensuring full self-consistency[44] have been explained in the previous work mentioned above. Basically, one chooses a convenient set of orthogonal functions, in this and most cases it is appropriate to take sine waves, and expands Eqs. (2.1) and (2.4) in terms of that set. The required matrix elements are the same as those used, for example, in Ref. 41 in the appropriate (nonmagnetic) limit. One assumes an initial form for the function $\Delta(z)$ and then iterates the process until self-consistency is achieved, that is, the $\Delta(z)$ function obtained from Eq. (2.4) is the same as the one input in Eq. (2.1) at the previous step.

Once self-consistency is achieved, one can directly examine quantities such as the pair potential $\Delta(z)$ and the Cooper pair amplitude $F(z)$ (also known as the condensation amplitude) where

$$F(z) = \Delta(z)/\lambda(z). \tag{2.5}$$

It is also very useful to examine, as a more accessible experimental quantity, the LDOS which is obtained from tunneling experiments, where the corresponding spectroscopic information can provided by scanning tunneling microscopy. We can express the LDOS $N(z,\epsilon)$ directly from the self-consistently calculated amplitudes $(u_{n\sigma}, v_{n\sigma})$ for the BdG Eqs. (2.1) as

$$N(z,\epsilon) = \sum_{\sigma} N_{\sigma}(z,\epsilon) = \sum_{\sigma,n} [u_{n\sigma}^2(z)\,\delta(\epsilon - \epsilon_n) + v_{n\sigma}^2(z)\,\delta(\epsilon + \epsilon_n)], \quad \sigma = \uparrow,\downarrow. \tag{2.6}$$

One can integrate $N(z,\epsilon)$ over a wide region of z to obtain the global DOS or over a very small region to obtain local results. Since our methods are free of any quasiclassical assumptions, our results are reliable even when the region examined is microscopic, i.e., on the order of the Fermi wavelength.

III. RESULTS

The results of our calculations are described in detail in this section. We will measure all the lengths in units of the Fermi wave vector k_{FS} in the S region, and define the relative dimensionless coordinate $Z \equiv k_{FS} z$. The thicknesses of the N and the S regions are taken to be, in these units, $D_N = D_S = 200$ while the superconducting coherence length (in the same units) is $\Xi_0 = 100$. Since $D_S = 2\Xi_0$, the pair potential rises to very close to its bulk value at the far edge of the superconductor. On the other hand, it does not decay all the way to zero in N: recall that the simplistic estimate[2] of the proximity depth is of order T_F/T (T_F is the Fermi temperature) in a clean system. It is obviously impractical for a numerical calculation to make the N slab thicker than this value, and it is not necessary either for our study, which focuses largely in the region near the interface. The values of $g = \equiv \lambda_N/\lambda_S$ studied are $g = 0, -1/3, -2/3, -4/5$. The values of the temperature are given in terms of the ratio T/T_c, where T_c is the bulk transition temperature in S. Most of the data presented here are at relatively low temperatures ($T = 0.1T_c$) but for most of the values of g we have obtained also results for reduced temperatures of 0.01, 0.2, and 0.3 and, in a few cases, up to 0.8 at 0.1 intervals. Values of the mismatch Λ [Eq. (2.3)] of 0.25, 0.5, 1, 2, and (in a few cases) 4 have been studied while for the barrier parameter H_B we have considered values of 0, 0.5, and 1.

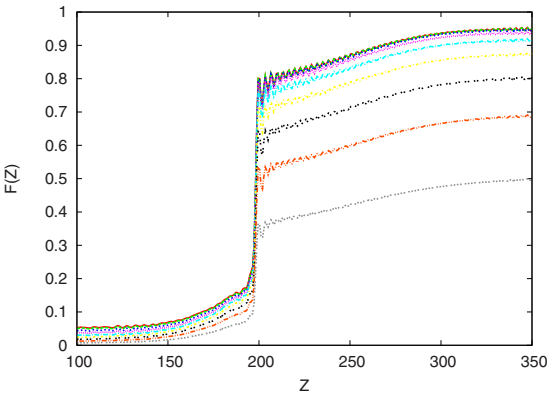

FIG. 1. (Color online) The spatial dependence of the normalized (see text) pair amplitude $F(Z)$. The dimensionless coordinate Z is in units of the Fermi wave vector in the S region ($Z \equiv k_{FS} z$). The interface at $Z_0 = 200$ separates the N region on the left with repulsive interaction ($g = -1/3$) from the S region on the right which has attractive superconducting coupling. The results are given for temperatures, expressed in terms of T_c, the transition temperature of bulk S, of T/T_c of 0.01, and 0.1 through 0.8, from top to bottom in the S region. The interfacial scattering $H_B = 1$ and the mismatch parameter $\Lambda = 0.5$ [Eq. (2.3)] correspond to a low-transparency junction.

In Fig. 1 we show that the behavior of the pair amplitude $F(Z)$ as a function of temperature is as expected. In this figure we have used values of $H_B = 1$ and $\Lambda = 0.5$ which correspond to strong interfacial scattering and high mismatch: hence a reduced proximity effect, as the N and S regions are weakly coupled. The value of g is intermediate, $g = -1/3$. $F(Z)$ is normalized so that its value in bulk S material at $T = 0$ would be unity. Results for temperatures from nearly zero to $0.8T_c$ at approximately equal intervals are shown. The range of dimensionless distance from the left edge $Z \equiv K_{FS} z$ includes one coherence length on the N side (at the left) and nearly all of the superconductor. The interface is (in all figures) at $Z \equiv Z_0 = 200$. We can see that $F(Z)$ rises toward the appropriate bulk value deep in S. Because of the strong scattering and high mismatch, the profile of $F(Z)$ near the interface is rather abrupt and the proximity effect overall, quite week compared with other cases discussed below. We see also that the temperature dependence of the proximity effect is in this case not very drastic [except as to the overall level of $F(Z)$] but appreciable.

In the next figure, Fig. 2, we discuss the influence of the interfacial scattering parameter H_B at a relatively high value of $|g|$ ($g = -2/3$) and, for clarity, in the absence of mismatch ($\Lambda = 1$). The quantity plotted this time is the pair potential $\Delta(Z)$ (the "order parameter") as a function of Z. $\Delta(Z)$ is normalized in the same way as $F(Z)$. Results for the three values of H_B studied are shown. In contrast to $F(Z)$, the pair potential in the N region will be negative for a repulsive interaction ($g < 0$). The negativity of $\Delta(Z)$ in N causes it to

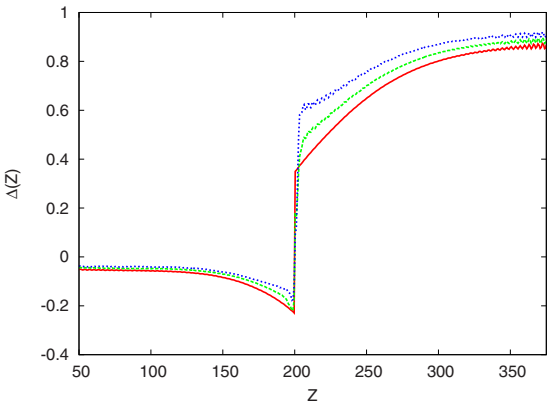

FIG. 2. (Color online) The spatial dependence of the pair potential $\Delta(Z)$ [normalized in the same way as $F(Z)$] for different values of the interfacial scattering H_B. From top to bottom, the results correspond to decreasing values of $H_B=1$ (blue), 0.5 (green), and 0 (red). $\Delta(Z)$ is calculated at low-temperature, $T=0.1T_c$, in the absence of mismatch, $\Lambda=1$, and for a strong repulsive interaction in the N region, $g=-2/3$.

abruptly jump at the interface. We see that this jump increases with H_B. This is as one would expect since higher barrier scattering isolates the S from the N material and leads to increased pair potential in S near the interface and to less leakage of Cooper pairs on the N side.

In a complementary way, for this two-parameter description (H_B,Λ) of the N/S interface, we show in Fig. 3, results for the effect of the mismatch parameter Λ at nonzero g ($g=-1/3$ in this case) at $H_B=0$. This time the quantity shown is $F(Z)$ (at smaller $|g|$ the N side the curves for $\Delta(Z)$ are harder to see). Results are shown for five values of Λ ranging from 1/4 to 4. It is evident that the proximity effect is dramatically enhanced when the absence of interfacial scattering is combined with the absence of mismatch ($\Lambda=1$), i.e., in the Cooper limit. Indeed, in this case [the (red) continuous curve] the behavior of $F(Z)$ at the interface is very smooth, without any sign of of abruptness. In the scale shown in the figure, and even at the finite temperature ($T=0.3T_c$) in the figure, the pair potential appears to settle into a constant on the N side.

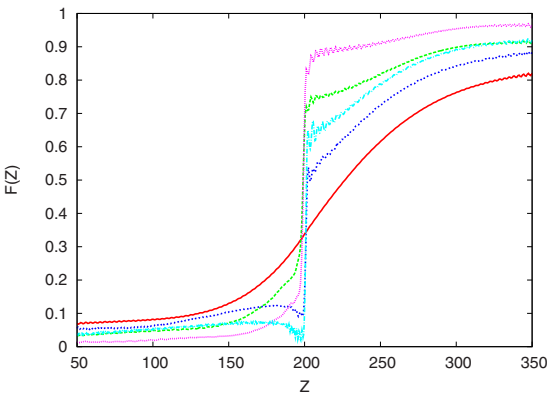

FIG. 3. (Color online) The spatial dependence of the pair amplitude $F(Z)$ for five different mismatch values $\Lambda=1/4$ (purple), 1/2 (green), 4 (cyan), 2 (blue), and 1 (red), from top to bottom on the right side. The results are given for $H_B=0$, $g=-1/3$ at $T=0.3T_c$.

This is of course not true: it keeps decaying but very slowly since the proximity depth is, in this case[2] much longer than the range shown in the figure and, indeed, longer than the numerical sample size.

In the previous two figures, Figs. 2 and 3, we have considered separately the influence of the parameters H_B and Λ. This is actually necessary: it is often assumed that these two parameters can be subsumed into a single parameter Z_{eff} that characterizes the effective barrier strength. In our notation, Z_{eff} (Ref. 45) would be related to H_B and Λ as

$$Z_{\text{eff}} = \left[\frac{H_B^2}{\Lambda^{1/2}} + \frac{(1-\Lambda^{1/2})^2}{4\Lambda^{1/2}} \right]^{1/2}. \tag{3.1}$$

It is instructive to relate this Z_{eff} to the normal-state junction transparency, i.e., the transmission coefficient of an N/N junction at normal incidence[10,43,45]

$$T_{NN} = 1/(1+Z_{\text{eff}}^2) \tag{3.2}$$

implying that $Z_{\text{eff}}=0$ (or, equivalently, $H_B=0$ and $\Lambda=1$) correspond to a completely transparent N/N junction while $Z_{\text{eff}} \gg 1$ would correspond to a very low-transparency (tunneling) limit. While such a single parameter (Z_{eff}) interface description offers a simplified approach and has been widely used, it may lead to even *qualitatively* incorrect trends, as compared to the correct description in which the effects of H_B and Λ are considered separately. This has been discussed in the context of F/S junctions[37,46] where it was possible to find an example in which the mismatch can actually *enhance* the junction transparency.[36,43,47–50]

Our results reveal that Z_{eff} alone is also inadequate to describe the proximity effects even in N/S junctions. Equivalently, just characterizing such junctions with either the corresponding transmission or reflection coefficient, as frequently done,[29] does not provide an unambiguous description. This can be clearly seen in Fig. 4, where two chosen pairs of (H_B,Λ) values [(0,1/2) and (0,2)] both yielding the same $Z_{\text{eff}}=0.174$ (an intermediate value also equivalent to $H_B=0.174$ and no mismatch, $\Lambda=1$) produce strikingly different results for both the spatial dependence of the pair amplitude and the local DOS. The two curves for $F(Z)$ display very different suppression near the interface in the S region and different decay in N. Analogous differences could also be observed for other pairs leading to the same or similar Z_{eff}. Clearly, the difference of calculated pair amplitudes which correspond to the same Z_{eff} also implies that other quantities such as the pair potential and the LDOS must also be inequivalent for the same Z_{eff}. This nonequivalence is clearly shown for the LDOS near the interface in the second panel of Fig. 4 for the same pairs of values (0,1/2) and (0,2). There we show the LDOS averaged over a region five Z units wide centered at $Z=205$, i.e., near the interface. The energy is in units of the bulk gap in S, Δ_0, and the LDOS is normalized to the value that it would have in an equivalent region in bulk S material: that is, the quantity plotted would be constant and unity in the normal state of bulk S material. These normalizations will be used in all LDOS plots below. The inequivalence is obvious. The results have very different peak positions and their heights are not at all the same. We

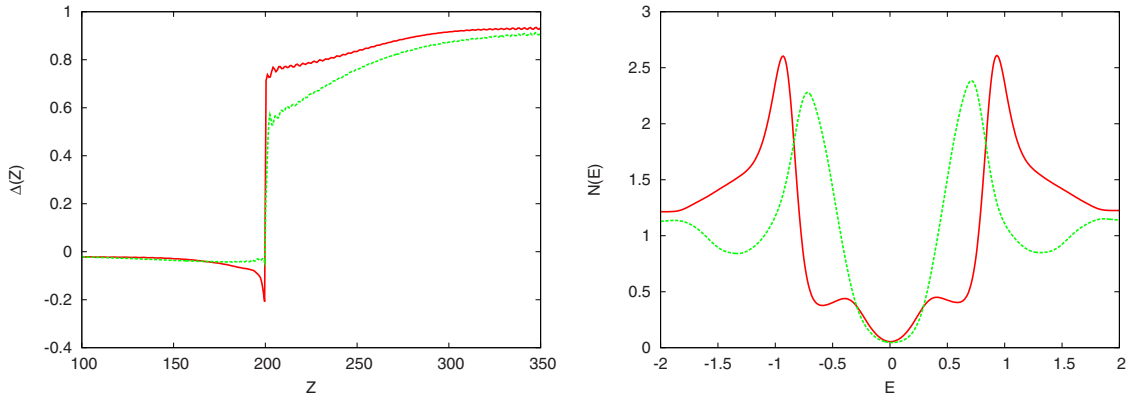

FIG. 4. (Color online) Comparison of results for two different pairs of interfacial scattering and mismatch values, $(H_B,\Lambda)=(0,1/2)$ and (0,2), which lead to the same effective barrier strength $Z_{\rm eff}$ [Eq. (3.1)]. The first panel shows $\Delta(Z)$. The top (red) curve at large Z is for the first set of values, the other (green) curve is for the second set. The right panel shows the LDOS $N(E)$ near (see text) $Z=205$. The energy E is in the units of the bulk zero-temperature superconducting gap Δ_0. $N(E)$ is normalized to its value in the normal state of the bulk S material (see text). The curve with the higher (red) peaks is the for first set of values and the lower (green) peaks are for the second set. The results in both panels, evaluated at $T=0.1T_c$ and $g=-1/3$, clearly show that $Z_{\rm eff}$ alone cannot describe the proximity effect or LDOS in N/S junctions.

find that this is true, in general. Only in a very crude sense are mismatch increases (that is, values of Λ different from unity) equivalent to increases in H_B, in that both lead to diminished proximity effect. With a little reflection, and perhaps some hindsight, one can realize that, since the nature of the surface scattering (normal or Andreev) originating from the mismatch is not the same as that arising from the barrier, the failure of this naive approximation should not have been so unexpected.

Returning now to the basic question of interest, the effect of the strength of the repulsive interaction in the N region, we show in Fig. 5 results for the pair amplitude $F(Z)$ for different values of the strength parameter g. For the results in this figure the values of $H_B=0$ and $\Lambda=1$ correspond to a transparent N/N barrier [recall Eqs. (3.1) and (3.2)], i.e., a very strong proximity effect. Another signature of this high transparency junction is the lack of Friedel oscillations, seen

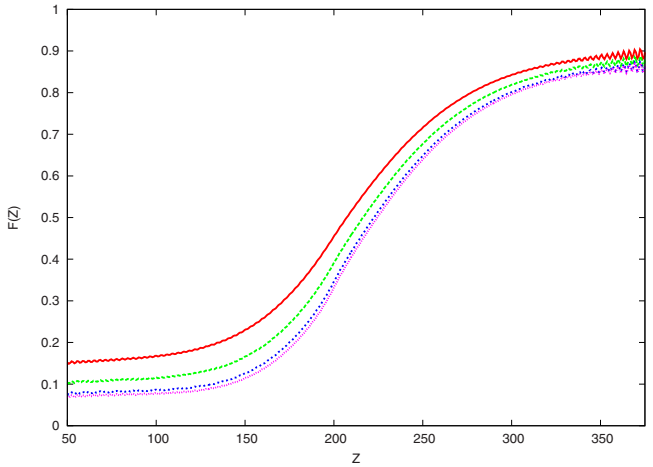

FIG. 5. (Color online) The spatial dependence of the pair amplitude $F(Z)$ for different values of the repulsive interaction in the N region: $g=0,-1/3,-2/3,-4/5$, from top to bottom. The results are given for $T=0.1T_c$, $H_B=0$ and $\Lambda=1$.

in the low-transparency case in Fig. 1. $F(Z)$ does not vanish even in the farthest region shown on the N (left) side and indeed, as expected, shows no sign of decay in the length scales shown. Toward the extreme right of the figure, nearly two coherence lengths in S, $F(Z)$ approaches in all cases its bulk value. However, looking in the regions near the interface and in the N region itself, we can clearly see how the proximity effect is strongly affected by g: the pair amplitude decreases with increasing $|g|$ not only in the entire N region but also in the S region within over one coherence length from the interface. Thus, as stated in the Introduction, the influence of a negative g pervades not only the N material but also a thick region in the superconductor, where the Cooper pair density is rather severely depleted.

We next examine the LDOS in the middle of the N and S region, about one coherence length away from each side of the N/S interface. The results are averaged over a region of width 100 centered in the middle of the N and S regions ($Z=100$ and $Z=300$, respectively). Energy and LDOS are normalized as explained in connection with Fig. 4. Panels (a) and (b) in Fig. 6 show the LDOS evolution with g, for the same parameters as used in Fig. 5. In both the N [panel (a)] and S [panel (b)] regions, $N(E)$ changes smoothly with g without the appearance of any new features, as compared to the $g=0$ limit (in the absence of any repulsive interaction). In this high transparency limit ($H_B=0$, $\Lambda=1$), there are strong proximity effects as can be seen in $F(Z)$ from Fig. 5. We therefore expect and find a g-dependent LDOS even one coherence length away from the interface, in both the N and S regions. We note that the LDOS at $E=0$ is appreciably larger in the N region. Increasing $|g|$ leads to larger LDOS values near $E=0$ while the peak near $E\pm0.5$ moves to slightly larger values of $|E|$. At $E=1$ there is a vestige of a peak on the S side, but not on the N side. This is of course reasonable, since such a peak exists in the bulk S, but not in the bulk N, material. In the panels (c) and (d) of Fig. 6 we consider the effect of the interfacial barrier strength on the LDOS, averaged in the same way, for a fixed $g=-2/3$. With increasing

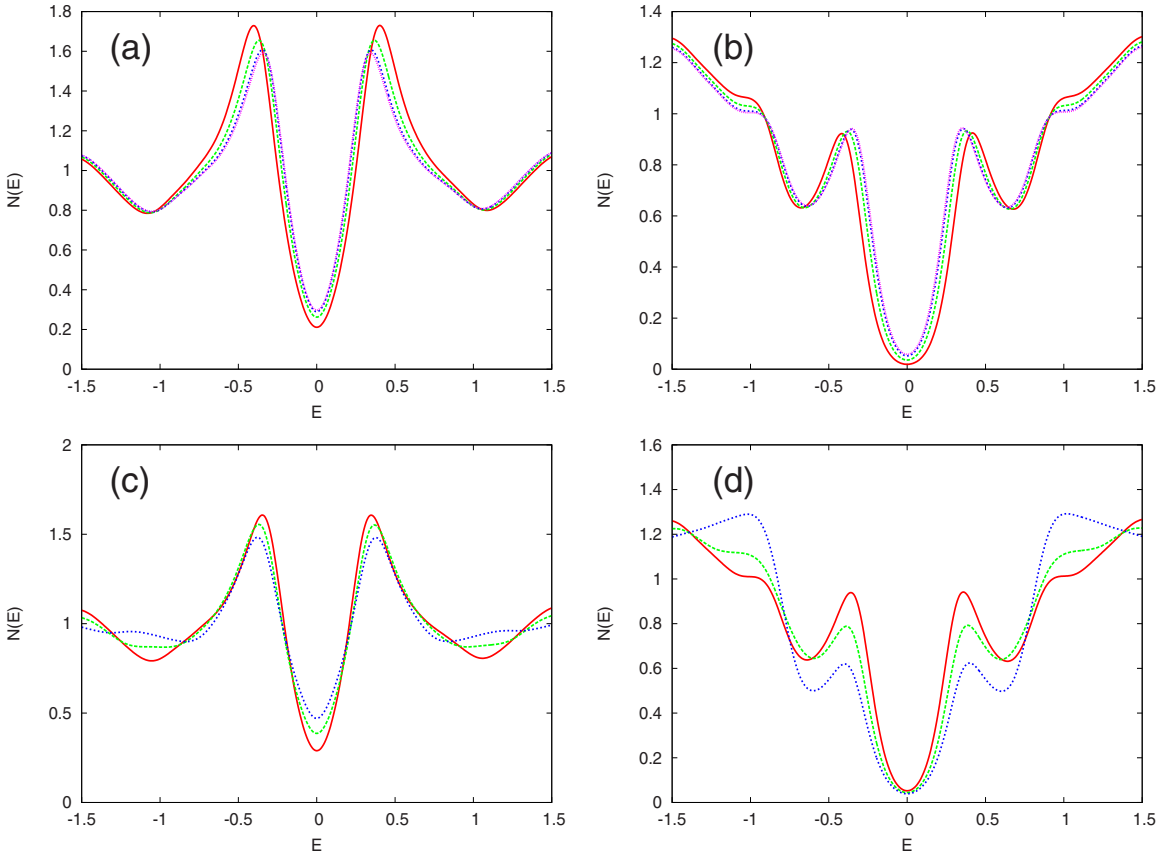

FIG. 6. (Color online) The LDOS $N(E)$ [Eq. (2.6)] in the middle region of the N and the S regions [centered at $Z=100$ and 300, respectively, and averaged over 50 Z units (see text)] at $T=0.1T_c$. Panels (a) and (b) show $N(E)$ for the N and S sides, respectively, at the same parameters used in Fig. 5: $H_B=0$, $\Lambda=1$, and $g=0,-1/3,-2/3,-4/5$, corresponding to curves (red, green, blue, and purple) for which $N(0)$ increases with $|g|$. Panels (c) and (d) similarly show the LDOS for the parameter values used in Fig. 2: $g=-2/3$, $\Lambda=1$, and three values of H_B, $H_B=0,0.5,1$ (red, green, and blue), LDOS peaks near $E=0.5$ are lower with increasing H_B.

H_B there is a suppression of the $N(E)$ peak at $E\approx\pm0.5$ in both the N and S electrodes but an increase in the peak at $E=1$ in the S side, as the proximity effect decreases. Near $E=0$ the LDOS is enhanced only in the N region. An increase in H_B diminishes the penetration of $\Delta(Z)$ in the N region and reduces its depletion in the S region (see Fig. 2) and this leads to the LDOS one coherence length away from the interface looking rather more bulklike as H_B increases. This effect is more marked if, in addition to increasing H_B, one sets $\Lambda\neq1$.

The effect of the repulsive interaction should be most pronounced close to the N/S interface. We focus next, therefore, on the spatial dependence of $F(Z)$ and $\Delta(Z)$ near the interface ($Z=Z_0=200$) as a function of g, in the low-temperature limit, $T=0.1T_c$. Panels (a) and (b) in Fig. 7 correspond to the high-transparency limit with $H_B=0$ and $\Lambda=1$ [recall that $Z_{\rm eff}=0$, from Eq. (3.1)]. As seen already in Fig. 5 [the (a) panel in Fig. 7 is a blow up of the interfacial region of Fig. 5], for every value of g $F(Z)$ gradually increases with Z and is smooth near the interface. In the limit of $g=0$ this behavior is well studied.[21,41] On the other hand, right at the interface, there is a strong suppression of $\Delta(Z)$, as compared to the bulk value. In the S region $\Delta(Z)$ and $F(Z)$ decrease very markedly with $|g|$ reflecting that the repulsive interaction in N induces a negative proximity effect in S. In the N region $\Delta(Z)$ is finite and negative for $g<0$: this sign change is reminiscent of the pair potential behavior due to the formation of π states at interfaces with unconventional superconductors or F/S junctions.[14,15,29,37,40,51–58] In this region, $|\Delta(Z)|$ increases with $|g|$ and decays away from the N/S interface. For $g\leq-2/3$, the length scale for this decay exceeds the superconducting coherence length. In the other two panels, (c) and (d), of Fig. 7 we consider, for comparison, parameter values in the low-transparency limit ($H_B=1$, $\Lambda=1/2$). In contrast to the other case, there is a much sharper, nearly discontinuous rise of $F(Z)$ with a steplike behavior near the interface, for every g. The rapid ($\sim k_F^{-1}$) oscillations that can be seen in the S region for both $F(Z)$ and $\Delta(Z)$ are not numerical artifacts but represent Friedel-type oscillations induced by the sharpness of the interface, which would not be seen in the quasiclassical treatment of this problem since such an approach would average over a k_F^{-1} length scale. As compared to the high-transparency limit, the two main differences that can be seen for $|\Delta(Z)|$ in Fig. 7 are that it attains a much higher value in both the N and S regions next to the interface; and that it decays much faster in the N region, away from the interface. This decay of $|\Delta(Z)|$ is in general nearly perfectly monotonic in both the high- and low-transparency limits. However, we have found some cases in which $F(Z)$ has a slight dip just inside the N region, next to

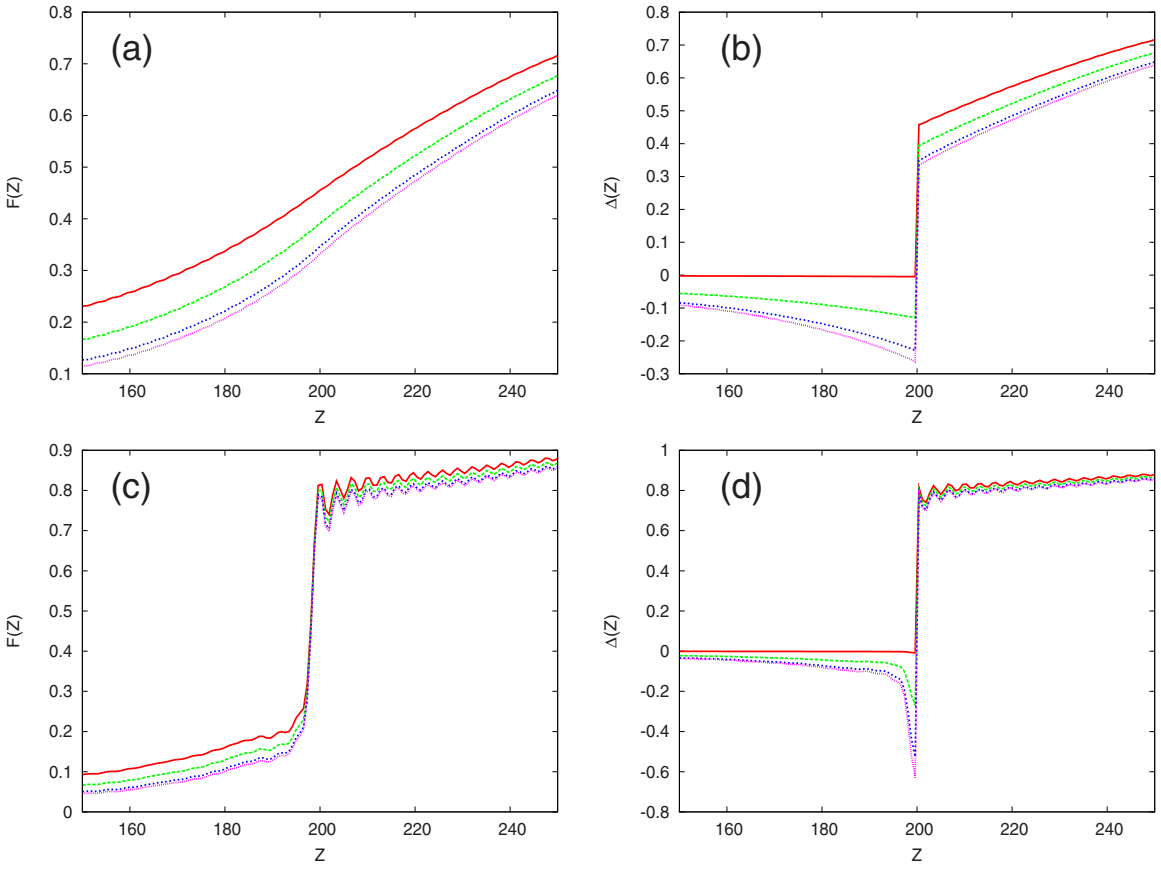

FIG. 7. (Color online) The pair amplitude $F(Z)$ and the order parameter $\Delta(Z)$ plotted in regions near the interface for four values of g, at $T=0.1T_c$. Panels (a) and (b) correspond to $H_B=0$, $\Lambda=1$ (high transparency) and panels (c) and (d) to $H_B=1$, $\Lambda=0.5$ (low transparency). In all cases lower values correspond to higher $|g|$. (red, green, blue, and purple curves correspond to $g=0,-1/3,-2/3,-4/5$, respectively)

the interface. This can occur when H_B is large (reflecting an interface scattering potential, averaged over a Fermi wavelength, of order of the Fermi energy) or in the presence of large mismatch (see, e.g., Fig. 3). In some cases this translates in $\Delta(Z)$ having a minimum slightly away from the interface. An example can be seen for $\Lambda=2$ in Fig. 4.

We explore further the interplay of strong proximity effects and the repulsive interaction in the N region by considering the interfacial LDOS at a region only one Z unit wide centered at $Z=201$, just one hundredth of a coherence length from the N/S interface, in the S region. The results shown in Fig. 8 are given for the high transparency H_B and Λ parameter values used in Figs. 6 and 7. Results at $Z=199$, just within the N region, are very similar. Comparing with the corresponding results in Fig. 6, we see that the results near the interface are qualitatively more similar to those well within (one coherence length) the N side than to those well within the S side, and exhibit the same trends. Quantitatively, however, there are large differences: the peaks near $E=0.5$, for example, are much more prominent at the interface. This is not really surprising: the pair amplitude is already drastically suppressed at the interface and (in this high-transparency case) it remains rather high in N even one coherence length away. The increased LDOS near the interface arises at least in part from additional Andreev-Saint James states. Interfacial π states have been shown to yield low-E LDOS peaks as observed in d-wave superconductors and attributed to the formation of Andreev bound states (ABS). Furthermore, even for N/s-wave-S junctions with a repulsive interaction in the N region, low-E LDOS peaks have been predicted using analytical but not self-consistent results [a step-function profile of $\Delta(Z)$] or employing quasiclassical approximations to calculate $\Delta(Z)$.[29,30] For example, for a

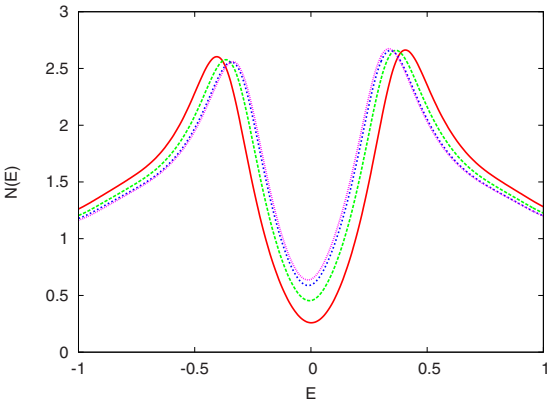

FIG. 8. (Color online) The local density of states very near the interface (a region one k_{FS}^{-1} unit wide centered at $Z=201$, one unit from the interface). At $Z=199$ the results are very similar. Results in this figure are for $H_B=0$, $\Lambda=1$ and (from bottom to top near $E=0$) are for increasing values of $|g|$ (red, green, blue, and purple curves correspond to $g=0,-1/3,-2/3,-4/5$, respectively).

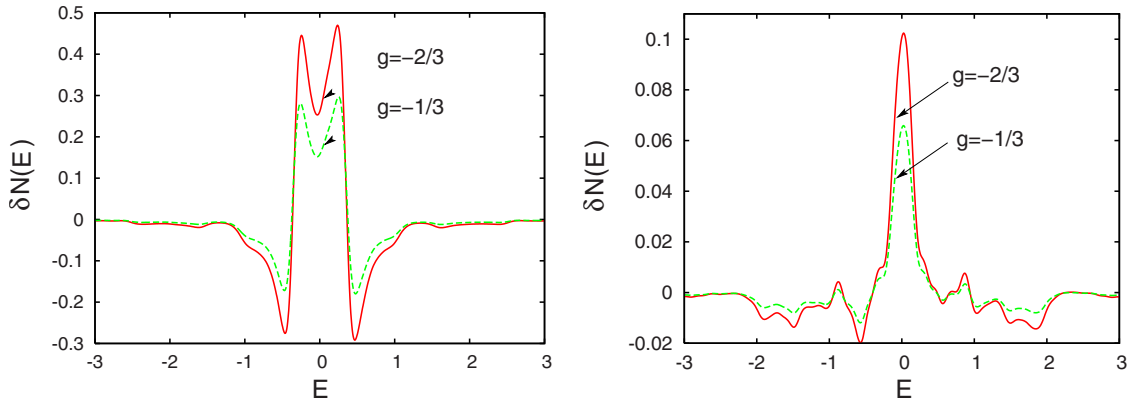

FIG. 9. (Color online) Difference between the normalized LDOS, $\delta N(E)$, near the interface ($Z=195$) at $g=0$ and $g<0$. The first and second panels correspond to a high- and low-transparency interface with $H_B=0$, $\Lambda=1$, and $H_B=1$, $\Lambda=0.5$, respectively.

spatial profile of $\Delta(z)$ qualitatively similar to the one we calculated in Fig. 2, the quasiclassical result of Ref. 30 (the inset of their Fig. 1) shows a very sharp zero energy LDOS peak. Our results show that, instead, the states at low energy are enhanced but the zero-energy peak is absent. This is often found theoretically[34,41] and experimentally[59,60] in F/S junctions. These results could reflect that the quasiclassical approximation can alter the exact position of the low-E interfacial LDOS peak for $g<0$.[61] We will further discuss the Z dependence of the LDOS in connection with Fig. 10 below.

To study in more detail the influence of g on the LDOS enhancement in the low energy region that we have observed, we subtract the corresponding $g=0$ LDOS near the interface from its $g\neq 0$ value. These normalized differences $\delta N(E)$ are shown in Fig. 9, which corresponds to LDOS results averaged over five Z units centered at $Z=195$. One can readily see that the effects of a nonzero g are quite significant in the low-energy region. The first panel corresponds to a high-transparency junction while the second panel is for a low-transparency case. We see that the increase of the LDOS with $|g|$ is largest in the region near $E=0$. The maxima are at $E=0$ in the low-transparency case and at nonzero E at high transparency. The latter situation has been also found to occur in LDOS or conductance results and attributed to unconventional pairing with broken time-reversal symmetry.[6,37,62–65] These peaks for the LDOS difference are clearly reminiscent of the peaks for the LDOS itself reported in quasiclassical studies for $g<0$ N/S junctions.[29,30] In the quasiclassical approximation, the peak position was studied as function of a reflection coefficient R that assumingly characterizes overall the specific N/S interface. The pitfalls of using a single parameter for such purposes have been exposed above and the use of quasiclassical methods to study very narrow spatial regions at the Fermi wavelength level is obviously suspect. It was expected that increasing R would shift the LDOS peak position from $E=0$ to finite E values.[29] Comparison with our rigorous, two parameter, results from Fig. 9, shows the opposite trend for the differential LDOS peak, which moves to $E=0$ with decreasing transparency. Our low-transparency differential LDOS results resemble the frequently observed LDOS zero-bias conductance peak, a signature of ABS in unconventional superconductors, which typically becomes narrower with the increase in Z_{eff} i.e., in R.[37] The trend we find, that a low-E the interfacial $\delta N(E)$ increases with g, is rather robust (we can see it for both high- and low transparencies and for a wide range of temperatures, not just $T\leq 0.1T_c$) and it is possible that it could be used to directly identify $g<0$ experimentally. Such an identification would be complicated by using the suitable $g=0$ LDOS background subtraction.

It is helpful to consider in more detail the behavior of the LDOS as one approaches the interface. While the existence of in-gap states is an inescapable consequence of the Andreev-Saint James surface states, neither experiment[59] nor theory[33,34] require that they be located at zero E. We now examine here how the position of the low-E LDOS peak depends on the LDOS location in the N/S structure and how this dependence changes as g varies and how this might correlate with the minimum in $\Delta(Z)$ being pushed away from the interface, as mentioned above. To elucidate this question, we consider the spatial evolution of the LDOS for both the $g=0$ and $g<0$ cases, as shown in Fig. 10. Results are given for the LDOS, evaluated at regions centered at distances 1, 3, 5, and 50 (in the usual units of k_F^{-1}), from each side of the N/S interface, and averaged over a region of the same total width as the corresponding distance from the interface. As always, we normalize the LDOS to the value it would have in an equivalent region of the bulk S material in its normal state. In the absence of a repulsive interaction [$g=0$, panels (a) and (b) for the N and S sides, respectively], moving away from the interface reduces the height of the low-E LDOS peaks (below $E\approx\pm 0.5$) in both the N and S regions. Near $E=0$ there is virtually no change in the N region [consistent with $\Delta(Z)=0$, for $Z<200$] while, on the other hand, there is a marked decrease in the zero-E LDOS as one moves away from the interface in the S region.

Comparison of these findings with those at $g=-2/3$ [panels (c) for the N side and (d) for the S side], reveals a similar LDOS structure but a different situation. While there are no new zero-E peaks, there are some clear differences. Near $E=0$ in the N region, moving closer to the interface does not lead to new LDOS peak formation, but we can notice a clear enhancement in the zero-E LDOS as the interface is approached from either side while the height of the low-E peaks increases very markedly as the interface is approached. On the S side of the interface, the low E peaks also increase

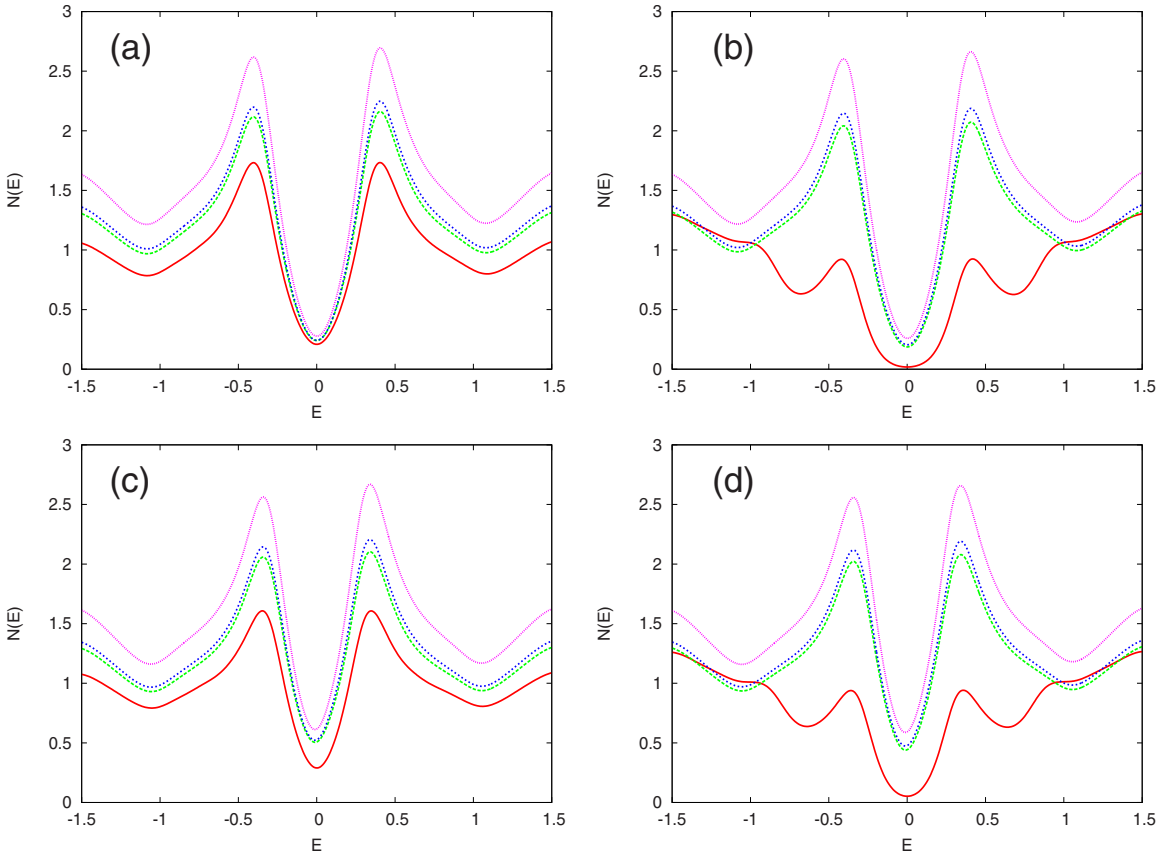

FIG. 10. (Color online) The local density of states for various distances from the interface in the high-transparency limit ($H_B=0$ and $\Lambda=1$) at $T=0.1T_c$, Panels (a) and (b) show results for the N and S regions of the sample respectively, at $g=0$, while (c) and (d) show results for $g=-2/3$. In all cases the ordering of curves, from top to bottom at $E=0.5$ corresponds to Z regions at distances, in units of k_F^{-1}, 1, 3, 5, and 50 (purple, blue, green, and red curves), from each side of the N/S interface, averaged over a region of the same total width as the distance from the interface.

as the interface is approached, and move slightly toward lower energies. We have observed similar trends in the LDOS for other junction parameters at other distances from the interface. In all those cases studied, we do not find a zero-E peak as was associated with ABS in the quasiclassical studies.[29] However, as can be seen from comparison of the N regions for $g=0$ and $g=-2/3$, the repulsive interaction leads to an enhanced low-E spectral weight. Subtraction of the LDOS, calculated close to the interface, for $g=0$ from that of $g=-2/3$ [(c) and (d) panels in Fig. 10] would again lead to a peak in the differential LDOS near $E=0$, as shown in Fig. 9. Thus, the observable effect of g is confirmed.

IV. CONCLUSIONS

While the possible role of a repulsive effective electron-electron interaction in the normal metal of a conductor/superconductor (N/S) junction, had already been noted in the early seminal work on the superconducting proximity effect,[22] subsequent studies almost universally considered such interaction to vanish identically. Perhaps the reason was that for the N/S proximity effect such a neglect leads to considerable simplifications. In the N region, the pair potential $\Delta(\mathbf{r})$ (the superconducting order parameter) vanishes identically and only the pair amplitude $F(\mathbf{r})$ needs to be considered. This leakage of Cooper pairs in the N region could then be approximately inferred by simply considering Andreev reflection and a step-function pair potential[10] although this would involve also neglecting the depletion of the pair potential in S. However, such assumptions, which would lead to the proximity effect being for many purposes independent on the choice of N material, could hardly be justified, theoretically or experimentally.

In this work, we have carefully and rigorously examined the various implications that the influence of a repulsive effective electron interaction in the N region has of the proximity effect in an N/S bilayer. In addition to the spatial variation of the pair amplitude, one also has to study the decay of the finite pair potential in N, away from the N/S interface, and its depletion in S. Each of those spatial dependences are strongly affected both by the effective interaction in N and by the N/S interfacial properties. In the N material, they have opposite trends in the magnitude: $F(z)$ is suppressed while $|\Delta(z)|$ is enhanced by a stronger repulsive interaction. In the superconductor, however, they are both depleted in the same way. This suppression of the pair potential near the interface is another signature of the proximity effect. It directly depends on the strength of this repulsive interaction. We also consider the dependence of the proximity effect on interface

scattering. Many studies of superconducting junctions employ a single-parameter description (for example, using the corresponding normal-state reflection or transmission coefficient) for the interface properties. We show explicitly that this is clearly insufficient, even for the commonly used δ-function model[10] of the interfacial barrier. More specifically, the nature of the proximity effect changes independently with *both* the strength of the interfacial barrier H_B and the Fermi wave vector mismatch Λ between the N and S regions.

We have not found any support for the formation of a zero-bias (or near zero bias) peak in the LDOS near the N/S interface, usually attributed to the formation of Andreev bound states. We do find a plethora of in-gap states attributable to these bound states in agreement with previous work. We find also similar zero E features for the differential LDOS, after performing a subtraction of the LDOS for vanishing repulsive interaction. Such differential LDOS peaks become more pronounced with increasing repulsive interaction and resemble the zero-bias conductance peaks studied extensively in unconventional superconductors.

A challenge for future work would be to identify specific materials and systems where the explored proximity effects could be readily observed. Our results show that, as might have been expected, the effects of a repulsive interaction are quantitatively important but not qualitatively obvious: there is no simple and evident "smoking gun." The peaks we find at small energies are in $\delta N(E)$ not in the local DOS itself. However, careful quantitative studies of the LDOS near the interface as a function of thickness should be (see, e.g., Figs. 8–10) revealing. Such studies have been technically possible for several years and have been found useful (see, e.g., Refs. 59 and 60) in the study of F/S systems. Furthermore, a repulsive interaction could be considered as a simple model for a strongly correlated N region. Materials such as VO or Pd could be used as the material forming the N layer, as well as other materials that may have an enhanced susceptibility, close to the Stoner instability. Such materials should have a repulsive effective interaction. Another direction would be to further examine semiconductors as the N region. Two classes of materials could be suitable candidates: ferromagnetic (II-I,Mn)V semiconductors, which have revealed unusual Andreev reflection in N/S junctions,[43,66,67] and nonmagnetic narrow-band gap semiconductors. In the second class, it might be useful to focus on InAs-based semiconductors. These materials offer high mobility and a suppressed Schottky barrier with S region and are already known for intriguing properties of Andreev reflection and proximity effects.[68] Gating of such a two-dimensional semiconductor would offer a natural path to alter the strength of the repulsive interactions.

Finally, recent experimental and theoretical advances could be used in the future to extend previous ideas about employing screening effects[25,26,28] to extract the strength of repulsive interactions in the N region. With an applied magnetic field the proximity induced superconductivity in the N region implies that there will also be a supercurrent and a Meissner effect. In the linear approximation for the Meissner effect (with the supercurrent proportional to the superfluid velocity), the presence of π states was associated with paramagnetic instability at N/S interface.[30] However, it has been shown that the region with suppressed pair potential can also lead to an important *nonlinear* contribution to the Meissner effect.[65,69] Revisiting the interplay of the screening response on the proximity effects could provide additional insights for probing repulsive interactions. Thus, there is reason to expect that additional ways of obtaining and interpreting experimental data in order to extract the effective pairing interaction will soon be available.

ACKNOWLEDGMENTS

We thank Paul H. Barsic for many conversations regarding his work and especially for developing most of the computer codes used to produce these result. This work was supported in part by NSF-ECCS CAREER, ONR, and AFOSR. I.Z. wishes to thank V. Lukic and J. Wei for discussions.

*Also at Minnesota Supercomputer Institute, University of Minnesota, Minneapolis, Minnesota 55455, USA; otvalls@umn.edu
†bryan175@umn.edu
‡zigor@buffalo.edu

[1] R. Holm and W. Meissner, Z. Phys. **74**, 715 (1932).
[2] G. Deutscher and P. G. de Gennes, in *Superconductivity*, edited by R. D. Parks (Dekker, New York, 1969), Vol. 2, p. 1005.
[3] E. L. Wolf, *Principles of Electron Tunneling Spectroscopy* (Oxford University Press, Oxford, 1985).
[4] B. Pannetier and H. Courtois, J. Low Temp. Phys. **118**, 599 (2000).
[5] A. M. Zagoskin, *Quantum Theory of Many-Body Systems* (Springer, New York, 1998).
[6] G. Deutscher, Rev. Mod. Phys. **77**, 109 (2005).
[7] P. G. de Gennes and D. Saint-James, Phys. Lett. **4**, 151 (1963).
[8] A. F. Andreev, Sov. Phys. JETP **19**, 1228 (1964).
[9] A. Griffin and J. Demers, Phys. Rev. B **4**, 2202 (1971).
[10] G. E. Blonder, M. Tinkham, and T. M. Klapwijk, Phys. Rev. B **25**, 4515 (1982).
[11] C. Bruder, Phys. Rev. B **41**, 4017 (1990).
[12] C. J. Lambert and R. Raimondi, J. Phys.: Condens. Matter **10**, 901 (1998).
[13] I. Bozović, G. Logvenov, M. A. J. Verhoven, P. Caputo, E. Goldobin, and T. H. Geballe, Nature (London) **422**, 873 (2003).
[14] A. I. Buzdin, Rev. Mod. Phys. **77**, 935 (2005).
[15] T. Kontos, M. Aprili, J. Lesueur, and X. Grison, Phys. Rev. Lett. **86**, 304 (2001).
[16] F. S. Bergeret, A. F. Volkov, and K. B. Efetov, Rev. Mod. Phys. **77**, 1321 (2005).
[17] E. A. Demler, G. B. Arnold, and M. R. Beasley, Phys. Rev. B **55**, 15174 (1997).
[18] Z. Radović, M. Ledvij, L. Dobrosavljevic-Grujić, A. I. Buzdin, and J. R. Clem, Phys. Rev. B **44**, 759 (1991); Z. Radović, L. Dobrosavljevic-Grujić, A. I. Buzdin, and J. R. Clem, *ibid.* **38**,

2388 (1988).
[19] I. Bozović, G. Logvenov, M. A. J. Verhoeven, P. Caputo, E. Goldobin, and M. R. Beasley, Phys. Rev. Lett. **93**, 157002 (2004).
[20] I. Asulin, A. Sharoni, O. Yulli, G. Koren, and O. Millo, Phys. Rev. Lett. **93**, 157001 (2004).
[21] M. Ashida, S. Aoyama, J. Hara, and K. Nagai, Phys. Rev. B **40**, 8673 (1989).
[22] P. G. de Gennes, Rev. Mod. Phys. **36**, 225 (1964).
[23] L. N. Cooper, Phys. Rev. Lett. **6**, 689 (1961).
[24] In the context of the preceding sentences, pages 1012–1019 of Ref. 2 are particularly relevant.
[25] G. Deutscher, Solid State Commun. **9**, 891 (1971).
[26] C. Vallette, Solid State Commun. **9**, 895 (1971).
[27] S. Wolf, G. Deutscher, and P. Lindenfeld, Solid State Commun. **10**, 909 (1972).
[28] G. Deutscher and C. Valette, in *Proceedings of the LT13 Conference*, edited by K. Timmerhaus, W. J. O'Sullivan, and E. F. Hammel (Plenum, New York, 1971), Vol. 3, p. 603.
[29] Y. Nagato and K. Nagai, J. Phys. Soc. Jpn. **64**, 1714 (1995).
[30] A. L. Fauchère, W. Belzig, and G. Blatter, Phys. Rev. Lett. **82**, 3336 (1999).
[31] Y. Blum, A. Tsukernik, M. Karpovski, and A. Palevski, Phys. Rev. B **70**, 214501 (2004).
[32] P. G. deGennes, *Superconductivity in Metals and Alloys* (Addison-Wesley, Reading, MA, 1989).
[33] P. H. Barsic, O. T. Valls, and K. Halterman, Phys. Rev. B **75**, 104502 (2007).
[34] K. Halterman, O. T. Valls, and P. H. Barsic, Phys. Rev. B **77**, 174511 (2008).
[35] Some of the challenges within the quasiclassical approach are related to the choice of the effective boundary conditions, not needed in our approach. See, for example, Ref. 21 and M. Ozana, A. Shelankov, and J. Tobiska, Phys. Rev. B **66**, 054508 (2002) which discuss possible discrepancies, larger than what would be expected by the accuracy of those methods.
[36] I. Žutić and O. T. Valls, Phys. Rev. B **60**, 6320 (1999).
[37] I. Žutić and O. T. Valls, Phys. Rev. B **61**, 1555 (2000).
[38] K. Halterman and O. T. Valls, Phys. Rev. B **70**, 104516 (2004).
[39] K. Halterman, P. H. Barsic, and O. T. Valls, Phys. Rev. Lett. **99**, 127002 (2007).
[40] K. Halterman and O. T. Valls, Phys. Rev. B **69**, 014517 (2004).
[41] K. Halterman and O. T. Valls, Phys. Rev. B **66**, 224516 (2002).
[42] In some of the literature, e.g., Ref. 22, the Cooper pair amplitude (condensation amplitude) is loosely called the order parameter. We are careful here to maintain the distinction between order parameter and pair amplitude according to Eqs. (2.4) and (2.5) below.
[43] I. Žutić and S. Das Sarma, Phys. Rev. B **60**, R16322 (1999).
[44] A description of the S region based on a step-function approximation for $\Delta(z)$ would not include signatures of the superconducting proximity effect, such as the suppression of the order parameter near the interface and a possible gap in the LDOS in the nonsuperconducting region. While such an approach does approximately retain superconducting correlations in the nonsuperconducting region, (see, e.g., Ref. 5), for a complete and accurate description self-consistency is essential.
[45] G. E. Blonder and M. Tinkham, Phys. Rev. B **27**, 112 (1983).
[46] P. H. Barsic and O. T. Valls, Phys. Rev. B **79**, 014502 (2009).
[47] Y. Zhu, Q. F. Sun, and T. H. Lin, Phys. Rev. B **65**, 024516 (2001).
[48] Z. Y. Zeng, B. Li, and F. Claro, Phys. Rev. B **68**, 115319 (2003).
[49] J.-F. Feng and S.-J. Xiong, Phys. Rev. B **67**, 045316 (2003).
[50] I. Žutić, J. Fabian, and S. Das Sarma, Rev. Mod. Phys. **76**, 323 (2004).
[51] C.-R. Hu, Phys. Rev. Lett. **72**, 1526 (1994); Phys. Rev. B **57**, 1266 (1998).
[52] S. Kashiwaya, Y. Tanaka, M. Koyanagi, H. Takashima, and K. Kajimura, Phys. Rev. B **51**, 1350 (1995); S. Kashiwaya and Y. Tanaka, Rep. Prog. Phys. **63**, 1641 (2000).
[53] K. Sengupta, I. Žutić, H.-J. Kwon, V. M. Yakovenko, and S. Das Sarma, Phys. Rev. B **63**, 144531 (2001).
[54] J. Y. T. Wei, N. C. Yeh, D. F. Garrigus, and M. Strasik, Phys. Rev. Lett. **81**, 2542 (1998).
[55] J.-X. Zhu, B. Friedman, and C. S. Ting, Phys. Rev. B **59**, 9558 (1999).
[56] S. Kashiwaya, Y. Tanaka, N. Yoshida, and M. R. Beasley, Phys. Rev. B **60**, 3572 (1999).
[57] K. Kikuchi, H. Imamura, S. Takahashi, and S. Maekawa, Phys. Rev. B **65**, 020508 (2001).
[58] Z. Y. Chen, A. Biswas, I. Žutić, T. Wu, S. B. Ogale, R. L. Greene, and T. Venkatesan, Phys. Rev. B **63**, 212508 (2001).
[59] N. Moussy, H. Courtois, and B. Pannetier, Europhys. Lett. **55**, 861 (2001).
[60] M. A. Sillanpää, T. T. Heikkila, R. K. Lindell, and P. J. Hakonen, Europhys. Lett. **56**, 590 (2001).
[61] M. B. Walker and P. Pairor, Phys. Rev. B **59**, 1421 (1999).
[62] M. Covington, M. Aprili, E. Paraoanu, L. H. Greene, F. Xu, J. Zhu, and C. A. Mirkin, Phys. Rev. Lett. **79**, 277 (1997).
[63] M. Fogelström, D. Rainer, and J. A. Sauls, Phys. Rev. Lett. **79**, 281 (1997).
[64] I. Žutić and I. Mazin, Phys. Rev. Lett. **95**, 217004 (2005).
[65] I. Žutić and O. T. Valls, Phys. Rev. B **56**, 11279 (1997).
[66] J. G. Braden, J. S. Parker, P. Xiong, S. H. Chun, and N. Samarth, Phys. Rev. B **91**, 056602 (2003).
[67] R. P. Panguluri, K. C. Ku, T. Wojtowicz, X. Liu, J. K. Furdyna, Y. B. Lyanda-Geller, N. Samarth, and B. Nadgorny, Phys. Rev. B **72**, 054510 (2005).
[68] T. Schäpers, *Superconductor/Semiconductor Junctions* (Springer, Berlin, 2001).
[69] D. Xu, S. K. Yip, and J. A. Sauls, Phys. Rev. B **51**, 16233 (1995).